arXiv:cond-mat/0512717v4 [cond-mat.str-el] 24 Mar 2006

Excitations in correlated superfluids near a continuous transition into a supersolid

Erhai Zhao and Arun Paramekanti
Department of Physics, University of Toronto, Toronto, Ontario M5S-1A7, Canada

We study a superfluid on a lattice close to a transition into a supersolid phase and show that a uniform superflow in the homogeneous superfluid can drive the roton gap to zero. This leads to supersolid order around the vortex core in the superfluid, with the size of the modulated pattern around the core being related to the bulk superfluid density and roton gap. We also study the electronic tunneling density of states for a uniform superconductor near a phase transition into a supersolid phase. Implications are considered for strongly correlated superconductors.

PACS numbers: 71.27.+a, 05.30.Jp, 03.75.Lm

The theoretical idea that ^{4}He could become a supersolid [1] at low temperature has motivated experimental studies of defect excitations in the solid phase [2], as well as a theoretical investigation of vortices in a superfluid near a first-order transition to a supersolid [3], as indirect windows into the proposed supersolid phase. Recent experimental hints [4] for a non-classical rotational inertia in solid ^{4}He have revived interest in this field. The copper oxide superconductors (SC) present a different situation, where the primary interest is in the uniform superconducting state, but it has long been recognized that the underdoped regime is plagued by various competing phases [5] involving spin, charge, and current ordering. Such competing phases can significantly affect the excitations in the superconducting state if there is a continuous transition between the uniform SC and these ordered phases. This is viewed as one possible cause for the anomalous excitation spectra of the underdoped cuprates. However, continuous phase transitions between phases with different order parameters are unusual and have only recently begun to be explored [6]. Further, recent tunneling experiments [7] in highly underdoped $Ca_{2-x}Na_xCuO_2Cl_2$ ($T_c \approx 10-20$K) suggest that the ground state in this regime may be a supersolid rather than an insulator. Motivated by this, we consider here a continuous transition between a superfluid (superconductor) and a supersolid, on a lattice, and explore some qualitative consequences for excitations in the uniform superfluid (superconducting) state near such a transition.

The following are our main results. (i) A continuous transition into a commensurate supersolid phase is known to arise, with increasing interactions, from condensation of rotons when the roton gap vanishes. Here, we show that alternatively a uniform current flow in the superfluid can also induce supersolid order by driving the roton gap to zero. (ii) This current-driven collapse of the roton gap results in a supersolid pattern emerging around the vortex core in the uniform superfluid as shown in Fig. 1. The length scale over which this modulation is significant is $R_v \sim D_s/E_{\rm rot}$, where D_s is the bulk superfluid stiffness and $E_{\rm rot}$ is the roton gap in the homogeneous superfluid. (iii) We use microscopic calculations and Ginzburg-Landau (GL) theory to obtain the long distance profiles of the modulated and uniform components of the density and superfluid order parameter around the vortex, as shown in Fig. 1. (iv) Finally, we ask whether tunneling into a uniform SC near a transition into a supersolid phase can probe the low energy roton excitations. Within a slave boson approach, we show that a tunneling electron can excite the bosonic condensate modes in the SC. In SCs with a small superfluid density, this leads to inelastic secondary peaks in the tunneling spectrum as shown in Fig. 2. Coherence factors however suppress contributions from wavevectors corresponding to the roton minimum. We conclude with possible implications for correlated SCs such as the doped cuprate materials.

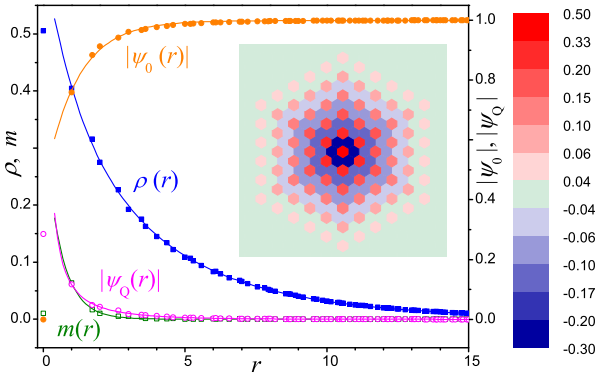


FIG. 1: (color online) Profiles of the modulated ($\rho, |\psi_{\mathbf{Q}}|$) and uniform ($m, |\psi_0|$) components of the density/superfluid order parameters around a vortex in a superfluid near a transition to a supersolid. Inset: Density modulations near the core.

Microscopic model and Landau theory: Consider a model of hard-core bosons with nearest-neighbor repulsion on the triangular lattice,

$$\mathcal{H} = -J_\perp \sum_{\langle i,j\rangle} \frac{1}{2}(b_i^\dagger b_j + \text{h.c.}) + J_z \sum_{\langle i,j\rangle} (n_i - \frac{1}{2})(n_j - \frac{1}{2}). \quad (1)$$

For large $J_\perp/J_z \equiv \Delta$ the ground state of this Hamiltonian is a uniform superfluid. In the interaction dominated regime, for $\Delta \lesssim 0.2$, quantum Monte Carlo simulations [8] have shown that the uniform superfluid

is unstable to density-wave modulations at wavevectors $\pm\mathbf{Q} \equiv (\pm 4\pi/3, 0)$, leading to a supersolid. Through the standard mapping $(S_i^+ = b_i^\dagger, S_i^- = b_i, S_i^z = n_i - 1/2)$, this Hamiltonian is equivalent to an $S = 1/2$ XXZ spin model with ferromagnetic in-plane interaction $J_\perp$ and an antiferromagnetic out-of-plane interaction J_z. Spin-wave calculations on this XXZ model [9], valid at large-S, show that the phase transition into the supersolid is caused by the vanishing of the roton gap at $\pm\mathbf{Q}$, which leads to roton condensation. They also capture the precise structure of the supersolid phase of model (1) which is now known from direct numerics for $S = 1/2$ [8]. Further, both techniques agree that the transition from the superfluid to the supersolid is *continuous* which is also indicated from a GL analysis outlined in Melko *et al.* [8]. Since we are interested in the consequences of a continuous superfluid to supersolid transition, we focus on this specific model. We will use (semi)classical analyses of the XXZ model, supplemented by GL theory, as a reliable guide to the physics of model (1).

Keeping the relevant wavevectors $\mathbf{q} = \mathbf{0}, \pm\mathbf{Q}$ to describe the superfluid to supersolid transition, the superfluid order, $\psi(\mathbf{r})$, and the deviation of the density from half-filling, $\delta n(\mathbf{r}) = n(\mathbf{r}) - 1/2$, can be expressed as $\psi(\mathbf{r}) \sim \psi_0(\mathbf{r}) + \psi_{\mathbf{Q}}(\mathbf{r})e^{i\mathbf{Q}\cdot\mathbf{r}} + \psi_{-\mathbf{Q}}(\mathbf{r})e^{-i\mathbf{Q}\cdot\mathbf{r}}$ and $\delta n(r) \sim m(\mathbf{r}) + \rho(\mathbf{r})e^{i\mathbf{Q}\cdot\mathbf{r}} + \rho^*(\mathbf{r})e^{-i\mathbf{Q}\cdot\mathbf{r}}$. The complex numbers $\psi_0, \psi_{\pm\mathbf{Q}}, \rho$ and the real number m are, thus, order parameters in the GL theory [8, 10, 11]. For the model (1), ψ_0 is nonzero in, both, the superfluid and the supersolid, while $\psi_{\pm\mathbf{Q}}, m, \rho$ are nonzero only in the supersolid. Since we are interested in a hard-spin formulation here, it is convenient to work with the phase and amplitude of the superfluid order parameters $\psi_0, \psi_{\pm\mathbf{Q}}$. Terms such as $\psi_{\mathbf{Q}}^2\psi_{-\mathbf{Q}}^*\psi_0^*$ and $\psi_{\mathbf{Q}}^*\psi_{-\mathbf{Q}}^*\psi_0^2$ in the GL functional lock the phases of these different components, so that $\psi_0 = |\psi_0|e^{i\varphi}, \psi_{\pm\mathbf{Q}} = |\psi_{\pm\mathbf{Q}}|e^{i\varphi}$ are determined by three amplitudes and a single phase variable φ. The amplitudes are constrained by the $|\psi_0|^2 + |\psi_{\mathbf{Q}}|^2 + |\psi_{-\mathbf{Q}}|^2 + m^2 + 2|\rho|^2 = 1$, which fixes the spin length (to unity).

The GL functional $f = f_\rho + f_m + f_\psi + f_c$, where

$$f_\rho = \alpha_\rho|\rho|^2 + g_\rho|\nabla\rho|^2 + u_\rho|\rho|^4 + w_\rho \mathrm{Re}(\rho^6)\ldots \quad (2)$$

$$f_m = \alpha_m m^2 + g_m(\nabla m)^2 + u_m m^4 \ldots \quad (3)$$

$$f_\psi = \varrho_s|\nabla\varphi|^2 + \ldots \quad (4)$$

$$f_c = -\lambda_1\varrho_s^2|\rho|^2|\nabla\varphi|^2 + \lambda_2 m\mathrm{Re}(\rho^3) + \lambda_3[\rho^2(\psi_{\mathbf{Q}}\psi_0^* + \psi_{-\mathbf{Q}}^*\psi_0) + \mathrm{c.c.}] + \lambda_4[m\rho\psi_{-\mathbf{Q}}\psi_0^* + \mathrm{c.c.}]\ldots \quad (5)$$

where we have only displayed terms relevant to our analysis below. These terms respect the particle-hole and lattice symmetries of the Hamiltonian in Eq. (1), and could be, in principle, derived using functional integral methods as outlined for a related model in Ref.[12]. Here we treat the coefficients as phenomenological parameters. In Eq. (2), $\alpha_\rho \equiv a(\Delta - \Delta_{c0})$ measures the distance to the superfluid-supersolid transition point with $a > 0$. Spin-wave theory and Monte Carlo calculations indicate $w_\rho < 0$, which prefers ρ to be real in the supersolid. In f_c, the term λ_1 couples the modulated solid order and the superflow current $\varrho_s\nabla\varphi$. The $\lambda_{2,3,4}$ terms induce effective "magnetic fields" upon the different order parameters.

Current driven collapse of the roton gap: For superfluids close to a supersolid instability, external perturbations that suppresses the kinetic energy relative to the interaction energy can drive the system into the supersolid phase. Consider a uniform superflow, say in the x direction, which introduces a phase difference between neighboring sites, $\delta = \phi_j - \phi_i$. The phase gradient effectively suppresses the nearest-neighbor kinetic energy from Δ to $\Delta\cos(\phi_i - \phi_j)$. Carrying through the calculation of spin-wave fluctuations around such a state with superflow, we find a spin-wave dispersion with a roton gap $\omega(\mathbf{Q}) = 1.5\sqrt{6\tilde{\Delta}(\tilde{\Delta} - 1/2)}$, where $\tilde{\Delta} \equiv \Delta[2\cos(\delta/2) + \cos\delta]/3$, reduced by the current flow. The point where the roton gap collapses is thus shifted upward to $\Delta_c \simeq \Delta_{c0}[1 + (\delta/2)^2]$, where in the last step we assumed $\delta \ll 1$. Recalling the current density $J \sim \sin\delta \approx \delta$, we conclude the boost of Δ_c is quadratic in the supercurrent density close to the transition, and the superflow induces supersolid ordering.

In the GL approach, superflow-induced supersolid ordering can be described phenomenologically by the coupling term λ_1 between the supercurrent and the supersolid order parameter ρ in Eq.(5). This term effectively shifts α_ρ to $\alpha'_\rho = \alpha_\rho - \lambda_1 J_s^2$, where the supercurrent $J_s = \varrho_s|\nabla\varphi|$. We thus see that one can induce a transition from a superfluid ($\alpha'_\rho > 0$) into a supersolid ($\alpha'_\rho < 0$) by a superflow which leads to a sufficiently large $|\nabla\varphi|$. The "critical current density" required to obtain the supersolid is $J_c = \sqrt{\alpha_\rho/\lambda_1}$. This is analogous to superflow induced spin-density modulation [13] and gradient couplings inducing competing phases [14] considered earlier only within GL theory. We next turn to implications of this for a vortex in the superfluid phase.

Vortex in the superfluid phase: For a superfluid vortex, the current density increases upon approaching the core as $J_s = \varrho_s/r$. The above result then indicates that the superflow would cause a supersolid pattern to be stabilized in a region with characteristic radius $R_v = \varrho_s\sqrt{\lambda_1/\alpha_\rho}$ around the core. It is clear from the GL functional that $\alpha_\rho \sim E_{\mathrm{rot}}^2$, since the roton gap determines the distance to the transition. We thus identify $R_v \sim \varrho_s/E_{\mathrm{rot}}$. We have confirmed this by microscopic calculations where we have evaluated the roton gap, the superfluid stiffness D_s (which has energy units and can be viewed as ϱ_s/m^* with an effective mass m^*) and the "critical current" using spin-wave theory.

To study, further, the interplay of the various order parameters near a vortex, we numerically studied model (1) in the presence of an orbital magnetic field, by replacing t in Eq. (1) with $t_{ij} = t\exp(i\int_j^i \mathbf{A}\cdot d\mathbf{l})$. We

considered an $L\times L$ lattice with periodic boundary conditions, and a vector potential corresponding to a uniform magnetic field with the total flux chosen to be one flux quantum. The ground state then corresponds to a single vortex within the cell. Transforming to an effective spin model, and treating the spins as classical unit vectors, we found the ground state spin configuration $\{\mathbf{S_r}\}$ using a simulated annealing algorithm. The ground state corresponds to a single vortex with its core on a site of the lattice. The local order parameters at each $\mathbf{r}$, i.e. ρ, m, ψ_0, and $\psi_{\pm\mathbf{Q}}$, were extracted from $\{\mathbf{S_r}\}$ by coarse graining over six nearest neighbor sites.

The inset to Fig. 1 shows the map of the boson density $\delta n(\mathbf{r})$ around a vortex for $\Delta = 0.505$ — it is clear from this that supersolid order is induced in the vicinity of the vortex core as expected from earlier arguments. Each data point in the plotted profiles in Fig. 1 represents the angular average taken at a fixed distance from the core. It is apparent that as the superflow induces a nonzero ρ, the order parameter $|\psi_0|$ is suppressed. At the same time, $|\psi_{\pm\mathbf{Q}}|$ and m are generated but they are insignificant except very near the vortex core. We explain these features below using GL theory.

Outside of a few lattice spacings from the vortex center $m \simeq 0, \psi_{\pm\mathbf{Q}} \simeq 0$ and we will ignore them to begin with. Assuming ρ is small, and $|\psi|$ is almost constant, the free energy density relevant to ρ reduces to $f_{\rm far} \approx (\alpha_\rho - \lambda_1 \varrho_s^2 |\nabla\varphi|^2)|\rho|^2 + g_\rho |\nabla\rho|^2 + u_\rho |\rho|^4 + \ldots$, where we have dropped the higher order w_ρ term but implicitly use $w_\rho < 0$ to consider only real ρ solutions below (the numerical solution for the vortex yields an almost purely real ρ). It is clear that for small r, $|\nabla\varphi| \sim 1/r$ is large and renders the state with $\rho = 0$ unstable. Minimizing f with respect to ρ^*, introducing $s(r) = \rho(r) 2u_\rho/\alpha_\rho$, one finds $s(r)$ obeys the differential equation $\xi_\rho^2[d^2s/dr^2 + (1/r)(ds/dr)] - s^3 + (R_v^2/r^2 - 1)s = 0$. Here $\xi_\rho = \sqrt{g_\rho/\alpha_\rho}$ is the coherence length for ρ, and $R_v = \varrho_s\sqrt{\lambda_1/\alpha_\rho}$ as defined before is the length scale associated with the supersolid order. The solution to this equation at large r is $s(r) \sim e^{-r/\xi_\rho}/\sqrt{r}$. This solution breaks down close to the vortex core as ρ saturates to a finite value at $r = 0$. The numerical result for $\rho(r)$ can be fit well over the region $r > 1$ with $\rho(r) = Ae^{-r/\xi_1}\tanh(\sqrt{\xi_2/r})$, as shown by the solid line in Fig. 1. The length scale $R_v \sim [\langle r^2\rho(r)\rangle/\langle\rho(r)\rangle]^{1/2}$, where the $\langle.\rangle$ denotes the spatial average with the vortex at the origin. Once we have a nonzero $|\rho|^2$ (far from the core) it suppresses, via the hard-spin constraint, the uniform superfluid order parameter $|\psi_0|^2$ with $\left[|\psi_0|^2 + 2|\rho|^2\right] \approx 1$ since $m, \psi_{\pm\mathbf{Q}} \simeq 0$. Next we turn to these order parameters which are small everywhere. We see from Eq. (5) that $\lambda_2 \mathrm{Re}(\rho^3)$ acts as a magnetic field for m, while $\lambda_3\rho^2\psi_0^*$ induces $\psi_{\mathbf{Q}}$. Thus we expect $m \sim \mathrm{Re}(\rho^3)$ and $|\psi_{\pm\mathbf{Q}}| \sim |\rho|^2|\psi_0|$ (except very close to the core), as borne out by our numerics.

Tunneling: We next analyze electron tunneling into the uniform SC to see if it probes the low-energy roton excitation when the system is on the brink of becoming a supersolid. We use a slave boson formulation, writing the electron operator as $c_\sigma(\mathbf{r},\tau) = f_\sigma(\mathbf{r},\tau)b(\mathbf{r},\tau)$ where f_σ is a spinful fermion (spinon) and b is a charged boson. Assuming that gauge fluctuations and interactions are innocuous in the superconducting state, the electron Green function can be factorized as $G^c_\sigma(\mathbf{r},\tau) = G^f_\sigma(\mathbf{r},\tau)G^b(\mathbf{r},\tau)$. In mean-field theory, when the boson is condensed, we can replace $G^b(\mathbf{r},\tau) \sim \langle b\rangle^2$, so that $G^c \sim G^f$, their ratio being the condensate density $\langle b\rangle^2$. The electron tunneling spectrum thus reflects the tunneling density of states (TDOS) associated with the spinon spectrum.

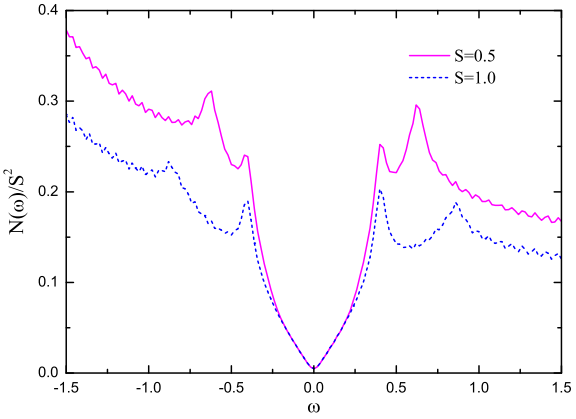


FIG. 2: Tunneling DOS for an f-wave triplet SC on the triangular lattice. We set the spinon hopping $t_f = 1$, the spinon pairing gap $\Delta_f = 0.4$, and set $J_\perp = J_z \approx 0.08$ in Eq. (1) for the condensate. Low energy roton modes do not influence the V-shaped nodal spectrum due to coherence factors. The lower energy peaks are elastic spinon peaks, secondary peaks arise from condensate fluctuations. At smaller S, the inelastic contribution is larger while the weaker condensate dispersion shifts the secondary peak to lower energy.

Going beyond mean field theory, we assume that the bosons are described by an interacting Hamiltonian such as (1) and evaluate the boson Green function using spin-wave theory. Combining this with the spinon Green function, for a model with spinon pairing, leads to the TDOS

$$N_c(\omega) = \frac{S^2}{V}\sum_{\mathbf{k}}\left(v_{\mathbf{k}}^2\delta(\omega + E_{\mathbf{k}}) + u_{\mathbf{k}}^2\delta(\omega - E_{\mathbf{k}})\right) \qquad (6)$$

$$+\frac{S}{2V^2}\sum_{\mathbf{q}\neq 0,\mathbf{k}}\gamma_{\mathbf{q}}^2\left[v_{\mathbf{k}}^2\delta(\omega + E_{\mathbf{k}} + \Omega_{\mathbf{q}}) + u_{\mathbf{k}}^2\delta(\omega - E_{\mathbf{k}} - \Omega_{\mathbf{q}})\right].$$

Here $u_{\mathbf{k}}^2, v_{\mathbf{k}}^2$ are the usual superconducting coherence factors associated with spinon pairing, while $\gamma_{\mathbf{q}}^2$ is the coherence factor associated with the Bogoliubov transformation for diagonalizing the boson model [15]. The first term, which dominates at large-S, reflects the mean field result where the condensate does not fluctuate. The second term represents inelastic processes where tunneling inserts a spinon and excites condensate fluctuations.

To show the effects of condensate fluctuations in a *nodal* SC on the triangular lattice, we plot in Fig. 2

the TDOS $N_c(\omega)$ obtained for f-wave triplet pairing of spinons [16]. The two main features of the spectrum in Fig. (2) are: (i) At low energy the nodal spectrum is nearly unaffected by the condensate fluctuations. (ii) At higher energies, condensate fluctuations lead to a broad secondary peak. This arises from $\mathbf{q}$ regions where there is a large density of states for condensate excitations. These remain true even in the presence of low-energy rotons since the $\gamma_{\mathbf{q}}^2$ coherence factor tends to reduce the contribution to the TDOS coming from near the roton wavevector $\mathbf{Q}$. The energy difference between "elastic" and "inelastic" peaks scales with the superfluid stiffness.

Experimental implications: Our results for the superflow induced supersolid, the vortex core size scaling and the existence of secondary tunneling peaks rely mainly on the existence of a continuous superfluid-supersolid transition and a small superfluid density, largely independent of the detailed microscopics. Here we consider some implications for the cuprate superconductors. Tunneling measurements on near-optimal superconducting $Bi_2Sr_2CaCu_2O_{8+\delta}$ ($T_c = 89$K) in a $B = 5$T magnetic field see a modulated TDOS around the vortex core [17]. Although different explanations have been proposed for this pattern (e.g., Refs.[20, 21, 22]), it is possible that over the large region (with radius ~ 75Å) in which the modulated pattern appears the system may be better viewed as a supersolid (which appears to be seen at low doping and $B = 0$ in a related cuprate [7]). If this supersolid has a charge modulation, the roton in this system at $B = 0$ could be observed using inelastic X-ray scattering. We expect that the roton energy should scale as $E_{\rm rot} \sim D_s/R_v$ where D_s is the bulk superfluid stiffness and R_v is the radius of the region around the vortex core exhibiting a checkerboard modulation. Further, the observed modulation region around the vortex core should grow with underdoping upon approaching the supersolid. Both predictions could be tested experimentally. We have also shown that condensate fluctuations can lead to inelastic secondary peaks at higher energies, while leaving the low energy V-shaped spectrum unaffected. This is broadly consistent with tunneling data in the cuprates where regions with a small superfluid density and broad secondary tunneling peaks (so-called "large gap" regions) coexist with "small gap" regions of larger superfluid density and single peaks [18]. However, the fact that the high energy structure carries information about the ordering wavevector in the cuprates [19] does not appear to be a feature of the model we have studied. This may need coupling to disorder which can simultaneously lead to low superfluid density and supersolid order in certain regions and also to scattering of quasiparticles off the disorder induced supersolid. Further, one needs to address possible bond-order instabilities [20, 23, 24]. We hope our work will also stimulate experiments to study supersolids and vortices [25] using cold atoms on optical lattices, and vortices in superfluid ^{4}He near freezing pressure.

We thank J.C. Davis, T. Hanaguri, H. Hoffman, H.-Y. Kee, Y.-B. Kim, Y.-J. Kim, S. Sachdev, A. Vishwanath, and Z. Wang, for useful discussions and correspondence. This work was supported by a startup grant and a Connaught grant from the University of Toronto.

[1] A.F. Andreev and I.M. Lifshitz, Sov. Phys. JETP **29**, 1107 (1969); G. Chester, Phys. Rev. A **2**, 256 (1970); A.J. Leggett, Phys. Rev. Lett. **25**, 1543 (1970).
[2] G. Lengua and J.M. Goodkind, J. Low Temp. Phys. **79**, 251 (1990).
[3] Y. Pomeau and S. Rica, Phys. Rev. Lett. **72**, 2426 (1994).
[4] E. Kim and M.H.W. Chan, Nature **427**, 225 (2004); E. Kim and M.H.W. Chan, Science **305**, 1941 (2004).
[5] For representative reviews, see S. Kivelson *et al.*, Rev. Mod. Phys. **75**, 1201 (2003); E. Demler *et al.*, *ibid* **76**, 909 (2004); L. Balents *et al.*, cond-mat/0504692; M. Franz *et al.*, Phys. Rev. B **66**, 054535 (2002); A. Melikyan and Z. Tesanovic, *ibid* **71**, 214511 (2005).
[6] T. Senthil *et al.*, Science **303**, 1490 (2004); L. Balents *et al.*, Phys. Rev. B **71**, 144508 (2005).
[7] T. Hanaguri *et al.*, Nature **430**, 1001 (2004).
[8] D. Heidarian and K. Damle, Phys. Rev. Lett. **95**, 127206 (2005); R. G. Melko *et al.*, *ibid* **95**, 127207 (2005); S. Wessel and M. Troyer, *ibid* **95**, 127205 (2005); M. Boninsegni and N. Prokofiev, *ibid* **95**, 237204 (2005).
[9] G. Murthy *et al.*, Phys. Rev. B **55**, 3104 (1997). Spin wave theory finds a supersolid phase for $\Delta < \Delta_{c0} = 0.5$.
[10] We are indebted to Ashvin Vishwanath for pointing out that $\psi_{\pm\mathbf{Q}}$ is nonzero in the supersolid and would be generated by the couplings $\lambda_{3,4}$ in the GL theory.
[11] In the XXZ language, these order parameters correspond to the spin components S^z, S^+, S^- at $\mathbf{q} = \mathbf{0}, \pm\mathbf{Q}$.
[12] E. Frey and L. Balents, Phys. Rev. B **55**, 1050 (1997).
[13] E. Demler *et al.*, Phys. Rev. Lett. **87**, 067202 (2001).
[14] Z. Nussinov *et al.*, cond-mat/0409474.
[15] The coherence factor $\gamma_{\mathbf{q}}^2 = (\cosh 2\theta_{\mathbf{q}} + \sinh 2\theta_{\mathbf{q}})$ with $\cosh 2\theta_{\mathbf{q}} = \epsilon_{\mathbf{q}}/\Omega_{\mathbf{q}}$ and $\sinh 2\theta_{\mathbf{q}} = \Delta_{\mathbf{q}}/\Omega_{\mathbf{q}}$, where $2\epsilon_{\mathbf{q}} = \sum_{\hat\delta}[J_\perp(2 - \cos\mathbf{q}\cdot\hat\delta) + J_z\cos\mathbf{q}\cdot\hat\delta]$, $2\Delta_{\mathbf{q}} = \sum_{\hat\delta}[(J_\perp + J_z)\cos\mathbf{q}\cdot\hat\delta]$, and $\Omega_{\mathbf{q}}^2 = \epsilon_{\mathbf{q}}^2 - \Delta_{\mathbf{q}}^2$. Here $\hat\delta$ are unit vectors joining nearest neighbors on the triangular lattice.
[16] Details of the spinon Hamiltonian are unimportant. Since Coulomb interactions could modify the condensate spectrum at small q, we impose $|\mathbf{q}| > q_c \sim 1$ in Eq. (6). We have checked that including the plasmon mode (dispersing as $\sim\sqrt{q}$) and summing over all $\mathbf{q}$ in Eq. (6) does not affect our results qualitatively.
[17] J.E. Hoffman *et al.*, Science **295**, 466 (2002).
[18] A.C. Fang *et al.*, Phys. Rev. Lett. **96**, 017007 (2006).
[19] K. McElroy *et al.*, Phys. Rev. Lett. **94**, 197005 (2005).
[20] L. Bartosch *et al.*, cond-mat/0502002.
[21] M. Franz *et al.*, Phys. Rev. Lett. **88**, 257005 (2002).
[22] S.A. Kivelson *et al.*, Phys. Rev. B **66**, 144516 (2002).
[23] D. Podolsky *et al.*, Phys. Rev. B **67**, 094514 (2003).
[24] H.D. Chen *et al.*, Phys. Rev. Lett. **93**, 187002 (2004).
[25] C. Wu *et al.*, Phys. Rev. A **69**, 043609 (2004).